Carbon dynamics in highly heterotrophic subarctic thaw ponds

T. Roiha[1,3], I. Laurion[2] and M. Rautio[1,3]

[1]Department of Biological and Environmental Science, 40014 University of Jyväskylä, Finland

[2]Centre Eau Terre Environnement and Centre for Northern Studies (CEN), Institut national de la recherche scientifique, Québec G1K 9A9, Canada

[3]Département des sciences fondamentales and Centre for Northern Studies (CEN), Université du Québec à Chicoutimi, Québec G7H 4W2, Canada

Correspondence to: M. Rautio (milla.rautio@uqac.ca)

Abstract

Global warming has accelerated the formation of permafrost thaw ponds in several subarctic and arctic regions. These ponds are net heterotrophic as evidenced by their greenhouse gas (GHG) supersaturation levels (CO_2 and CH_4), and generally receive large terrestrial carbon inputs from the thawing and eroding permafrost. We measured seasonal and vertical variations in the concentration and type of dissolved organic matter (DOM) in five subarctic thaw (thermokarst) ponds in northern Quebec, and explored how environmental gradients influenced heterotrophic and phototrophic biomass and productivity. Late winter DOM had low aromaticity indicating reduced inputs of terrestrial carbon, while the high concentration of dissolved organic carbon (DOC) suggests that some production of non-chromophoric dissolved compounds by the microbial food web took place under the ice cover. Summer DOM had a strong terrestrial signature, but was also characterized with significant inputs of algal-derived carbon, especially at the pond surface. During late winter, bacterial production was low (maximum of 0.8 mg C m^{-3} d^{-1}) and was largely based on free-living bacterioplankton (58%). Bacterial production in summer was high (up to 58 mg C m^{-3} d^{-1}), dominated by particle-attached bacteria (67%), and strongly correlated to the amount of terrestrial carbon. Primary production was restricted to summer surface waters due to strong light limitation deeper in the water column or in winter. The phototrophic biomass was equal to the heterotrophic biomass, but as the algae were mostly composed of mixotrophic species, most probably they used bacteria rather than solar energy in such shaded ponds. Our results point to a strong heterotrophic energy pathway in these thaw pond ecosystems, where bacterioplankton dominates the production of new carbon biomass in both summer and winter.

1 Introduction

Traditional view of inland waters as sinks of carbon has changed during the past decades, and at present, lakes and ponds are considered net sources of carbon to the atmosphere (Tranvik et al., 2009). Increasing attention has been given to thaw ponds and lakes after recognizing the cumulative effect of their high abundance and greenhouse gas (GHG) emissions on global warming (Kling et al., 1992; Walter et al., 2006; Laurion et al., 2010), especially when they emit old carbon thus having the potential to act as a positive feedback mechanism on climate (Walter Anthony et al., 2014). Thaw ponds and lakes are dominant in continuous and discontinuous permafrost areas, for example in permafrost regions of Siberia where they represent 90% of all lakes (Walter et al., 2006), but until recently, little has been known on the limnological properties and microbial communities of this important freshwater ecosystem (Vonk et al., 2015).

Subarctic thaw ponds can be highly turbid and have relatively high nutrient concentrations (Breton et al., 2009; Rautio et al., 2011a) compared to most high latitude freshwater ecosystems (Pienitz et al., 1997; Hamilton et al., 2001; Medeiros et al., 2012). Moreover, high perimeter/volume ratio, the presence of palsas and bogs and the thawing of organic-rich permafrost in their watershed favor high inputs of dissolved organic matter (DOM) to the ponds. Chromophoric DOM (CDOM) can influence water column temperature regimes through its absorption of sunlight (Caplanne and Laurion, 2008), and with suspended particles, they contribute to form a distinct and stabile thermocline (Laurion et al., 2010). The rate of DOM input to aquatic systems has been documented to increase in boreal lakes over the last decades (Hudson et al., 2003), and while no such information is yet available for thaw ponds, the recent mobilization of terrestrial carbon stocks stored for thousands of years in the permafrost (Vonk et al., 2012) suggests a similar DOM increase is taking place also in the North.

High DOM concentration also strongly regulates the depth of the euphotic zone. Light is usually limited to the first meter in thaw ponds (Squire and Lesack, 2003; Watanabe et al., 2011), therefore restricting the water volume where photosynthesis can occur. This type of environment favors heterotrophic bacterial production (BP) that was shown to reach similar rates as in eutrophic lakes (Breton et al., 2009). The limnological characteristics of thaw ponds are likely also beneficial to mixotrophic algae and heterotrophic protozoans, as flagellated species are generally well adapted when lakes are rich in humic compounds (Jones, 2000). In low light conditions they can utilize

bacteria as an energy source, and as they are motile they also benefit from the nutrient-rich bottom waters (Arvola et al., 1991). They have been shown to be a key link in the carbon transfer from low to high trophic levels in small boreal forest lakes (Salonen and Rosenberg, 2000).

Circumpolar thaw ponds are ice covered for a large fraction of the year, which further affects carbon cycling, and generates large seasonal variations. The aim of this study was to demonstrate the difference in GHG accumulation, CDOM characteristics, and autotrophic and heterotrophic carbon pools between two seasons and depths. Comparisons were made between late winter and summer, and between surface and bottom waters in summer. We hypothesized that in the absence of light in winter or in the aphotic summer hypolimnion, autotrophic productivity stops while respiration continues, resulting in large summer and winter storage of GHG in the water column. We further hypothesized that the thermal structure in summer generates an accumulation of organic carbon in the hypolimnion where heterotrophy dominates. This study follows earlier ones looking at the limnological characteristics and bacterial communities of subarctic thaw ponds in summer (Breton et al., 2009; Negandhi et al., 2013; Rossi et al., 2013; Crevecoeur et al., 2015).

2 Methods

2.1 Sample collection and limnological analyses

The study was carried out in the discontinuous permafrost region near the village of Whapmagoostui-Kuujjuarapik (55° 20’ N 77° 30’ W), Northern Quebec, Canada, along the River Kwakwatanikapistikw (local Cree name; KWK is used to name the ponds hereafter) where a large number of thaw ponds can be found. At this site, ponds are thermokarstic and form over an impermeable clay-silt bed, preventing most hydrological interactions among ponds, on center of thawed lithalsas (or inorganic palsas). They are surrounded by dense shrubs and sparse trees, and occasional areas of mosses and aquatic plants. More details on the study area are provided in Bouchard et al. (2014) and Bouchard et al. (2011).

Five ponds were studied during late winter (6-11 April) and summer (8-14 August) in 2009. They are all small (averaged diameter 17 m ± 1.3 m) and shallow (average depth 2.5 m ± 0.4 m). Sampling was done with a Kemmerer water sampler (Wildco® USA) through a borehole drilled into the ice in winter, and from an inflatable boat in summer at the middle of the pond. During

winter sampling, the water started pouring over the ice through the hole because of the pressure from the weight of snow and ice, and possibly resulting in a mixing of surface with deeper water. This was suggested as the factor explaining the similar GHG concentrations obtained in surface (just under the ice) and bottom waters (approximately 0.5 m above the sediments), despite the expected inverse thermal stratification at this period of the year (Laurion et al., 2010). All other samples were collected from about 1 m below the ice and considered as representative of an integrated water column. In summer, surface and bottom waters were sampled from just below the surface and approximately 0.5 m above the bottom sediments.

Measures of temperature, dissolved oxygen, pH and conductivity were done with a 600R YSI multiparametric probe (Yellow Springs Inc.). Further analyses were performed on water prefiltered through a 50-µm sieve. Total suspended solids (TSS) were obtained by filtering 500-1000 mL of water onto precombusted and preweighted GF/F filters (Advantec MFS Inc.). The 50-µm prefiltration reduced the TSS by an average 5.8% in comparison to bulk water samples, both analyzed in summer (data not shown). Filters were stored at -20°C until they were dried for 24 h at 60°C, and weighted to get sestonic dry weight or TSS. They were subsequently combusted at 450°C for 2 h to be able to calculate the organic fraction of TSS. An aliquot of water was filtered through a pre-rinsed cellulose acetate filter (0.2 µm pore size; Advantec MFS Inc.) to analyse soluble reactive phosphorus (SRP; unpreserved samples) and iron (Fe; samples preserved with HNO_3 at 0.15% final concentration). Total phosphorus (TP) and total nitrogen (TN) were analysed from unfiltered water preserved with H_2SO_4 (final concentration of 0.15%). All nutrient samples were stored in acid-washed glass bottles in dark and cold (4°C) until further analysis as in Breton et al. (2009).

2.2 Carbon characterization

Dissolved CO_2 and CH_4 were determined as in Laurion et al. (2010). In brief, 2 L of pond water were equilibrated into 20 mL of ambient air for 3 min, with the headspace sampled in duplicated glass vials (Vacutainers©) previously flushed with helium and vacuumed. Gas samples were analyzed by gas chromatography (Varian 3800), and dissolved gas concentrations were calculated according to Henry's Law.

The water filtered through pre-rinsed cellulose acetate filters as above was also used to analyze dissolved organic carbon concentration (DOC), and for optical analyses of CDOM. Samples were

stored in amber glass bottles in dark and cold (4°C) until the analysis. DOC was quantified using a carbon analyzer (Shimadzu TOC-5000A) calibrated with potassium biphthalate. The absorbance was measured from 200 to 800 nm with a spectrophotometer (Varian Cary 300), using 1-cm quartz cuvettes on dual-beam mode, at 1 nm intervals for winter samples, and 4 nm intervals for summer samples. Null-point adjustment was performed using the mean value from 750-800 nm, and the absorption coefficients (a_λ) were calculated from absorbance measurements (A_λ) at 254 and 320 nm using $a_\lambda = 2.303\ A_\lambda/L$, where L is the length of the cuvette in meters (Mitchell et al., 2002). The absorption coefficient at 320 nm (a_{320}) was used as an index of CDOM concentration. Specific UV absorbance–index ($SUVA_{254}$) was determined from DOC normalized A_{254}, and used as an index of aromaticity (Weishaar et al., 2003).

CDOM absorption spectra were further analyzed to calculate the spectral slopes S_λ (Loiselle et al., 2009) between 250 nm and 450 nm (Galgani et al., 2011). Slopes were calculated over 20 nm intervals with a 1 nm step (i.e. 250-269, 251-270,…) for winter samples, and 4 nm steps for summer samples (i.e. 250-269, 254-273,…). The resulting set of spectral slopes was plotted by center wavelengths. Calculations were performed in open source software package SciLab 4.15. The individual spectral slope S_{289} was used to evaluate the amount of fulvic and humic acids likely related to the autochthonous production (Loiselle et al., 2009). Algal-derived carbon has a maximum slope at 289 nm, while terrestrial carbon spectral slopes lack this peak and present a spectrally variable distribution with a steady increase from 260 to 390 nm.

2.3 Microbial abundance and productivity

For the determination of chlorophyll *a* (Chl-*a*) concentrations, 1-2 L of 50 µm-sieved pond water were filtered onto GF/F filters. Samples were collected in duplicates and stored at -80°C until pigment extraction and fluorometric analysis were done in hot ethanol according to Nush (1980). Water samples for the enumeration of nanoflagellates (PNF: phototrophic and mixotrophic cells; HNF: heterotrophic cells) and phototrophic picoplankton (PPA) were preserved with 0.2 µm-filtered glutaraldehyde solution at a final concentration of 1%. Three replicate aliquots (3-5 ml) were filtered through 0.6 µm black polycarbonate filters (Nuclepore). Samples were stained with 4-,6-diamido-2-phenylindole (DAPI), mounted to slides and stored at -20°C until counting under UV excitation with an epifluorescense microscope (Zeiss Axiovert 200) at 1000× magnification.

Discrimination between pigmented and heterotrophic nanoflagellates was done with green excitation light. At least 50 cells or a maximum of 30 fields were counted from each sample. Nanoflagellate cells were further divided into three size categories: < 5 µm, 5-10 µm and > 10 µm. Volumes were converted to carbon biomass using the carbon content coefficient of 0.19 pg C μm^{-3} for PNF and HNF (Putt and Stoecker, 1989). Phototrophic picoplankton carbon content was calculated using the carbon conversion equation (pg C = $0.433 \times V^{0.866}$, where V is in μm^3) for picoeukaryotic cells (Verity et al., 1992; Campbell et al., 1994).

Bacterial abundance (BA) was measured with a flow cytometer (FACSCalibur, Becton-Dickinson) as in Rossi et al. (2013) before and after sonication to obtain estimations of free-living and particle-attached bacterial abundance. Biomass calculation for bacterioplankton was based on biovolumes measured from digital images acquired from DAPI-stained microscope slides using the *Cell C* program (Selinummi et al., 2005). Average bacterial carbon content was first estimated with allometric conversion formula recommended for DAPI stained cells (fgC = $218 \times V^{0.86}$, where V is in μm^3) (Posch et al., 2001). The average cellular carbon content (18.1 fg C $cell^{-1}$) was then multiplied by the bacterial abundance.

Bacterial production was measured from unfiltered and filtered (3 µm) water samples using tritiated leucine (^{3}H-leucine) incorporation with centrifugation (Smith and Azam, 1992). A solution of ^{3}H-leucine (specific activity of 164 Ci $mmol^{-1}$) was added to each vial to obtain a final leucine concentration of 30 nM, at which bacteria were saturated (experimentally tested). During the winter, the samples were incubated at ~0°C in the dark for 2 hours. During the summer, samples were incubated at *in situ* temperatures (5-18°C), depending on ponds. BP was stopped by adding trichloroacetic acid (5% final concentration), and samples were then stored at -20°C before the centrifugation step. Winter samples were radioassayed with a Perkin Elmer Tri-Carb 2800, and summer samples with a Beckman LS 6500. Leucine incorporation was converted to carbon biomass using coefficients from Simon and Azam (1989). Bacterial respiration (BR) was estimated from BP according to Del Giorgio and Cole (1998) BR model II.

Primary production (PP) was measured from the mixed water column during winter and from the surface in summer. An incubation system generating a gradient of photosynthetically active radiation (PAR), introduced by Rae and Vincent (1998), was used to obtain photosynthesis versus irradiance curves from complete darkness to full sunlight (E_{max}). The value for E_{max} was calculated

from *in-situ* PAR measurements available from a weather station located in Whapmagoostui-Kuujjuarapik, and assuming the air-water surface in these humic waters to cause a 50% decrease in radiation levels (Doxaran et al., 2004). A water volume of 20 mL was inoculated with a working solution of [^{14}C]-HCO_3 (80 µCi ml^{-1}) to a final concentration of 0.2 µCi ml^{-1}. In winter, the incubations were done outside (~0°C) under natural light conditions in a water bath for 45-60 min, while in summer a circulating water bath was used to keep samples at *in situ* temperature (14 – 18 °C) and incubations were run for 120 min. The incubations were terminated by filtrating samples onto GF/F filters, the method only capturing ^{14}C fixed in particulate organic matter and not the carbon allocated to exudates. The filters were subsequently frozen before they were radioassayed with a Perkin Elmer Tri-Carb 2800 liquid scintillation counter. Chl-a normalized carbon fixation rates were fitted to the equation of Platt et al. (1980) or Jassby and Platt (1976) depending on the presence or absence of photoinhibition, respectively. Data fit to the equations had on average a r^2 value of 0.92, and always higher than 0.81. The iterative non-linear regression of SigmaPlot 11.0 was used to obtain the maximum photosynthetic rate (P_{max}). PP at the pond bottom was estimated from the photosynthesis-irradiance curves and PAR estimated from in situ surface measurements, and diffuse attenuation coefficients calculated from a linear regression using TSS and DOC (Watanabe et al., 2011). Without light under the ice and snow cover, PP was established at zero. Light was measured under the ice with a Li-Cor Li-192 submersible PAR Quantum sensor.

2.4 Data analysis

Differences in environmental and microbial variables among waters were tested using a one-way ANOVA (fixed factor; JMP software, version 11.0.0, SAS Institute Inc. 2013). Conductivity, BP, PPA, SRP, and PNF biomass were log-transformed, while TP, TN, and BB were square-root transformed to achieve normality and homogeneity of variance in residuals (visually checked with predicted values). When differences were detected, a Tukey HSD multiple comparison test was performed. Environmental variables are illustrated with a principal component analysis (PCA) (PAST version 2.17c), where biological variables were entered as vectors which length and direction were determined by Spearman's correlation analysis between biological variables and PCA axis 1 and 2. Correlations between organisms (abundance, biomass and productivity measurements) and environmental variables were tested with non-parametric Spearman's rank

correlation coefficient analysis (IBM SPSS statistic 20.0). A significant level of $\alpha = 0.05$ was used for all statistical tests.

3 Results

3.1 Physicochemical properties of thaw ponds

In late winter, the ponds were covered with 50 to 70 cm of snow and approximately 30 to 60 cm of ice, which absorbed all light. Water temperature was 2.0°C under the ice and the ponds were likely O_2 depleted at the bottom because of the smell of hydrogen sulfide, while O_2 concentration was 4.5 ± 3.5 mg L^{-1} in the integrated water column sample. In summer, despite their shallow depth, ponds are strongly stratified with nearly 10°C difference in temperature and 10 mg L^{-1} difference in O_2 between surface and bottom (Fig. 1). Some ponds (KWK 2, 6 and 20) had a thermally homogenous epilimnion until 1 to 1.5 m depth, while in KWK 12 and 23 the temperature declined nearly linearly towards the bottom with a rate of 1-2°C every 50 cm. The pH varied between 6.0 and 7.5, with lowest and highest values respectively measured in summer bottom and surface waters. There was no difference ($p = 0.9034$) in conductivity between winter (50 ± 7 µS/cm) and summer at the surface (46 ± 10 µS/cm), but bottom waters had significantly ($p < 0.009$) higher conductivity (194 ± 67 µS/cm) than winter and summer surface waters. Nutrients were relatively high in all samples. TN concentrations were elevated in winter (958 ± 235 µg N L^{-1}) compared to the summer values (264 ± 118 µg N L^{-1}) ($p = 0.0001$). TP was relatively high in winter (97 ± 43 µg P L^{-1}), and in summer the concentrations were clearly lower at the surface (55 ± 29 µg P L^{-1}) than at the bottom (3110 ± 1043µg P L^{-1}) ($p = 0.0001$). SRP was available during the whole year, with higher concentrations in late winter (26 ± 15 µg P L^{-1}) and summer bottom waters (31 ± 36 µg P L^{-1}) than in summer surface where concentrations were relatively low (3.1 ± 3.0 µg P L^{-1}) but not statistically different from the other values ($p = 0.064$). All ponds had higher TSS in bottom waters (85 ± 43 mg L^{-1}), while in winter and summer surface waters the concentrations were generally an order of magnitude lower. In most ponds, organic fraction of TSS followed the same trend as TSS and made on average 24% of TSS. Fe was lower at the surface (0.3 ± 0.1 mg L^{-1}) than at the bottom of ponds (3.1 ± 1.6 mg L^{-1}) in summer. No Fe measurements were done during late winter. Limnological properties of the ponds are summarized in Table 1.

3.2 Carbon characterization

CO_2 and CH_4 concentrations were high in winter (up to 357 and 14.1 µM respectively), and particularly high at the pond bottom in summer (up to 815 and 312 respectively; Table 2). Surface waters, in contact with the atmosphere, had one order of magnitude lower concentrations, but values remained supersaturated. The inverse relationship ($r = -0.9228$; $p < 0.0001$) between O_2 and CO_2 suggests that the CO_2 originated from O_2 respiration and not from external sources such as weathering, runoff and groundwater inputs that are unlikely in the studied ponds. DOC ranged from 4.1 to 10.5 mg L^{-1}, with the highest concentrations obtained in winter. Despite the higher DOC observed in winter, CDOM was lowest at this period, as indicated by a_{320} values (7.1 ± 2.5 m^{-1} compared to 27 ± 10 and 70 ± 37 m^{-1} at the surface and bottom in summer, respectively). $SUVA_{254}$ followed the same trend as a_{320}, with lower values in winter (0.8 ± 0.2 L mg C^{-1} m^{-1}) compared to summer surface (4.8 ± 1.0 L mg C^{-1} m^{-1}) and bottom waters (7.7 ± 2.4 L mg C^{-1} m^{-1}), indicating the presence of more aromatic compounds, and possibly DOM-Fe complexes in summer. The shape of absorption spectral slopes showed a clear maximum at 382 nm, indicating the presence of terrestrial fulvic and humic acids. Consistent with the $SUVA_{254}$ index, S_{382} values were relatively low in winter (0.0137 ± 0.0016 nm^{-1}), with similar values in summer surface waters (0.0158 ± 0.0014 mg nm^{-1}), but show significant difference with bottom waters (0.0169 ± 0.0007 nm^{-1}) ($p = 0.0061$). The individual spectral slope S_{289} indicates that higher amounts of algal-derived carbon were present in summer surface waters (0.0148 ± 0.0009 nm^{-1}), especially in the most transparent pond KWK6 (0.0162 nm^{-1}), while their role was limited in the dark habitats under the ice (0.0113 ± 0.0011 nm^{-1}) and in bottom waters (0.0112 ± 0.0007 nm^{-1}). Carbon quantity and CDOM quality properties are summarized in Table 2, and the seasonal differences in absorption spectral slopes are shown in Fig. 2.

3.3 Microbial abundance and productivity

The abundance of all organisms examined was highest in the summer bottom waters, but the magnitude and seasonal distribution differed among taxa and ponds (Table 3). Especially, the abundant motile PNF accumulated in the nutrient-rich bottom waters, where their abundance was in most ponds an order of magnitude higher than at the surface (110 ± 89 vs. 27 ± 8 × 10^6 L^{-1}). The less abundant HNF also favored the bottom waters, with an order of magnitude difference in the

abundance between bottom and surface waters (9.2 ± 11.6 vs. 0.8 ± 0.7 × 10^6 L^{-1}). The smaller phototrophic picoplankton (PPA) and bacteria were more uniformly distributed, although the abundances were significantly higher ($p < 0.05$) at the bottom. Abundance was also quantified for free-living and particle-attached bacteria. During late winter, 74 ± 9% of bacterioplankton was attached to particles, and 46 ± 21% and 70 ± 17% in summer surface and bottom waters (Table A1).

When converted to biomass, the seasonal and vertical distribution pattern was even more accentuated (Table 3, Fig. 3). Overall, lower biomasses were encountered in winter, and higher at the bottom of the water column in summer. Total phototrophic biomass as Chl-*a* concentration (5.6 ± 2.5 µg L^{-1}) as well as the PNF biomass (152 ± 68 µg C L^{-1}) under the ice were relatively high. Summer surface phototrophic biomass was similar to winter waters ($p = 0.1213$), and it was different ($p < 0.05$) and highest in the dark bottom waters, likely reflecting cell sedimentation. The biomass of strictly phototrophic PPA was very low in winter (5.8 ± 4.4 µg C L^{-1}) and an order of magnitude higher in summer. The bacterial biomass was always high when compared to literature, with the lowest biomass occurring in winter (109 ± 67 µg C L^{-1}), two times higher biomass in summer at the surface (223 ± 36 µg C L^{-1}), and five times higher at the bottom (520 ± 146 µg C L^{-1}). The HNF contributed little to the total microbial biomass, especially in the illuminated summer surface waters where they averaged 3.2 ± 2.9 µg C L^{-1}. Their biomass was higher at the bottom (39.2 ± 49.4 µg C L^{-1}) and in winter samples (8.9 ± 4.7 µg C L^{-1}).

Snow and ice cover prevented light penetration under the ice, and therefore we assumed that no PP occurred *in situ* in late winter. However, the photosynthetic capacity of late winter phytoplankton community was not null, and represents the potential at the ice-out, which took place 2-3 weeks later. The maximum photosynthetic rate (P_{max}) of late winter phytoplankton community was for most ponds an order of magnitude lower than P_{max} of the summer community (2.0 ± 2.1 vs. 30.6 ± 26.1 mg C m^{-3} d^{-1}). BP rates were very low in winter (0.4 ± 0.2 mg C m^{-3} d^{-1}) and different ($p = 0.0001$) compared to the summer when surface (31 ± 14 mg C m^{-3} d^{-1}) and bottom (42 ± 19 mg C m^{-3} d^{-1}) BP rates. BR rates calculated from BP were low in winter (2.0 ± 0.6 mg C m^{-3} d^{-1}) and equally high during summer in surface (28 ± 6 mg C m^{-3} d^{-1}) and in bottom (33 ± 6 mg C m^{-3} d^{-1}). Particle-attached bacterioplankton played an important role in pond production at both sampling seasons (late winter: 42 ± 20%; summer surface: 66 ± 20%; bottom: 68 ± 44%; Table A1).

Winter, surface and bottom environmental characteristics formed three distinct groups on the PCA (Fig. 4a), with the first two axes explaining 72.9% of the variation in the environmental variables (PC1 46.0% and PC2 26.9%). Axis PC1 has strong positive correlations with TP (r=0.91), a_{320} (r=0.80), TSS (r=0.83) and GHG (CO_2 r=0.92 and CH_4 r=0.90), and strong negative correlations with pH (r=-0.81) and S_{289} (r=-0.65), whereas PC2 has positive correlation with temperature (r=0.81), S_{382} (r=0.69) and $SUVA_{254}$ (r=0.76), and negative correlation with TN (r=-0.93) and DOC (r=-0.67). Heterotrophs (BB and HNF) were correlated with PC1 while phototrophs (PP, PNF and PPA) were more strongly correlated to PC2 (Fig. 4b). Further, BP and BB were best correlated with carbon quality indices a_{320}, $SUVA_{254}$, and S_{289}, while HNF were best correlated with conductivity (Table 4). PP, PNF and PPA were best correlated with a combination of carbon quality indices, DOC and nutrients (Table 4).

4 Discussion

The large variations in physicochemical characteristics of thaw ponds between late winter and summer and between surface and bottom waters were reflected in their ecological properties. The cold and nutrient-rich winter waters had the lowest microbial abundance and productivity. The warm and illuminated summer surface waters favored primary production, while the colder and darker bottom waters accumulated nutrients, carbon compounds and microorganisms. The overall supersaturation in GHG and the clear dominance of heterotrophy over phototrophy, as expressed in the biomass and activity of the microbial food web components, indicate that the majority of the energy was flowing through the heterotrophic food web.

4.1 Spatial and seasonal variations in GHG

Greenhouse gas storage in pond waters occurred in winter under the ice cover and in summer under the steep thermocline, due to the isolation of these water masses from atmospheric venting. Partial pressures measured were especially large in summer hypolimnetic waters (in average 13 674 µatm of CO_2 and 4783 µatm of CH_4) compared to values at the surface (in average 1206 µatm of CO_2 and 9 µatm of CH_4). Such heterogeneity in the vertical distribution of GHG is typical for seasonally stratified lakes where bottom values are often many folds higher than at the surface (Eller et al.,

2005; Guérin et al., 2006; Bastviken et al., 2008). Partial pressures of CO_2 at the surface of thaw ponds (598-1545 µatm) were comparable to values obtained in other regions, for example in European boreal lakes (990 µatm; Kortelainen et al. 2006), Canadian boreal streams and rivers (1850 µatm; Teodoru et al. 2009), Western Siberian lakes and ponds (1935 µatm; Shirokova et al. 2012), or Canadian subarctic and arctic ponds (1896 µatm; Breton et al. 2009). Surface water CH_4 partial pressures (6-13 µatm) were also in the same range as values reported in lakes and ponds from North-America (11-59 µatm; Bastviken et al. 2008) Finland (23 µatm; Juutinen et al. 2009), Canadian Subarctic and Arctic (22 µatm; Breton et al. 2009), and Western Siberia (30 µatm; Shirokova et al. 2012).

The dominance of BR over PP, combined with the isolation of water masses during the long winter, followed by a very short spring mixing period (Laurion et al., 2010) and the steep summer stratification of these ecosystems controlled the accumulation of GHG in the hypolimnion. When normalized by the duration of the known isolation period (Laurion et al., 2010), GHG accumulated more rapidly in summer at the pond bottom (6.8 ± 2.2 µM CO_2 d^{-1} and 1.9 ± 0.9 µM CH_4 d^{-1}) than in winter under the ice cover (1.5 ± 0.3 µM CO_2 d^{-1} and 0.030 ± 0.027 µM CH_4 d^{-1}), assuming a constant accumulation rate during the two sampling periods and excluding freezing exclusion effects. This may be partly due to the more abundant microbial community in summer, although most GHG produced likely came from benthic respiration, especially in such shallow systems (Kortelainen et al., 2006). Summer also provides fresh organic matter that may stimulate GHG producers that indeed presented higher respiration rates. The smaller CH_4 accumulation rates in winter might also result from more optimal conditions for methanotrophy under the ice cover where bubbling CH_4 is trapped and dissolves in water. The amount of CH_4 in a lake was shown to depend on the size of the anoxic layer (Fendinger et al., 1992; Bastviken et al., 2004), and in the present study, this layer represents a particularly large proportion of the water volume in summer. During the autumnal turnover period (lasting about 2 months), the whole water column becomes oxygenated, and in the first part of the winter surface layer of the pond may contain sufficient oxygen (Deshpande et al., 2015) for efficient CH_4 consumption. Anoxic methanotrophy has also been reported (Sivan et al., 2011) and may occur at our study sites. Nevertheless, these GHG storage periods indicate that subarctic thaw ponds will release large amounts of CH_4 during the autumnal mixing period, and also during spring turnover if it lasts long enough (Walter et al., 2006; Laurion et al., 2010).

4.2 Seasonality in CDOM properties

We used a_{320} as an indicator of the quantity of CDOM, and $SUVA_{254}$, S_{289} and S_{382} as indicators of the aromatic content of CDOM and the relative proportions in allochthonous (terrestrial) versus autochthonous (algal) carbon sources. The high a_{320} and $SUVA_{254}$ values indicate a large contribution by terrestrial humic substances in DOM at the surface of thaw ponds in summer, with values similar to a few years earlier in the same ponds (Breton et al., 2009; Watanabe et al., 2011). CDOM values were clearly smaller in winter (late winter a_{320}; Table 2) and less aromatic ($SUVA_{254}$) than in summer, suggesting that carbohydrates or protein-like compounds from bacteria-induced CDOM-degradation made up a larger fraction of DOM in winter. Laurion et al. (unpublished data) tested the role of bacterial CDOM degradation in arctic thaw ponds and found that its importance can almost match that of photodegradation in certain cases, without significant losses in DOC, potentially indicating a bacterial transformation into less colored compounds. The higher DOC values observed in winter (average of 8.3 mg L^{-1}) compared to summer at the surface (5.8 mg L^{-1} in) thus likely resulted from a combination of a generation of dissolved compounds from the uninterrupted but slower microbial activity, and out-freezing inputs associated to the formation of ice. Although BP in late winter was low, the long subarctic winters allow accumulation effects that could lead to a decrease in CDOM. The labile part of DOC is known to be consumed within days by bacterioplankton, leaving the recalcitrant fraction of DOC to dominate in environments where fresh inputs are limited (Del Giorgio and Davis, 2002; Roehm et al., 2009; Guillemette and del Giorgio, 2011). However this is not clearly observed in the present study thaw ponds, where less aromatic and non-chromophoric fractions increased along winter, likely as the result of DOM recycling by a rich microbial food web, together with a lack of new carbon inputs from the frozen catchment.

The high a_{320} and $SUVA_{254}$ values found in bottom waters are very likely caused by the elevated dissolved iron concentrations (up to 5.1 mg L^{-1}; r^2 = 0.947 between $SUVA_{254}$ and Fe in summer samples, n=10). High concentrations of iron (>2 mg L^{-1}) were shown to form complexes with humic substances and increase DOM absorbance (Maloney et al., 2005; Xiao et al., 2013). During the autumnal turnover, CDOM-Fe complexes from bottom waters are exposed to photochemical reactions at the surface, potentially generating hydroxyl radicals that dissociate carboxyl groups

393 from humic substances. These reactions can lead to lower molecular weight carbon components at
394 the same time as increasing the water clarity (Brinkmann et al., 2003). The spectral slope values
395 indicate that algal-derived proteins (S_{289}; Galgani et al. 2011) were more abundant in summer
396 surface waters when primary production and Chl-*a* were highest, and at the same time fulvic and
397 humic acids (S_{382}) also seemed more abundant than in winter. Algal proteins are generally highly
398 available to heterotrophic organisms and were likely supporting the higher summer BP (Kritzberg et
399 al., 2004). Nevertheless, Xiao et al. (2013) showed how high Fe concentrations, such as found in
400 bottom waters, can significantly lower DOM absorption slopes, thus interpretations of bottom water
401 S_λ should be done cautiously.

402

403 **4.3 Thaw pond microbial food web**

404 Primary production rates in summer at the surface of thaw ponds were in the same range as in other
405 arctic and subarctic lakes (Lizotte, 2008), while in late winter snow and ice cover prevented *in situ*
406 PP. However, when exposed to light, the production of carbon by the winter phytoplankton
407 community was in the same range as the heterotrophic production, suggesting that the high
408 phytoplankton biomass encountered during late winter were made of mixotrophic species that
409 switched from hetero- to autotrophic production at ice-out. Similarly, the high Chl-*a* and PNF
410 biomass in the light-limited bottom waters in summer were most likely composed of mixotrophs.
411 Many species of Chrysophycaea, Cryptophyceae and Dinophyceae are known to be 99%
412 mixotrophic (Olrik 1998 and references therein). Chrysophyceae were dominating the
413 phytoplankton community in KWK2 and KWK20 (Dupont 2008, L. Forsström, unpublished data).
414 Many Chrysophyceae species have flagella, and thus can thrive in sheltered humic ponds that have
415 been shown to favor diurnal migrations of phytoplankton (Jones, 1991). This is especially
416 advantageous in steeply stratified and shallow ponds where phytoplankton can migrate within a few
417 hours (Arvola et al., 1991), and are able to use nutrient-rich hypolimnetic waters (Salonen et al.,
418 1984). The high nutrient concentrations in bottom waters likely explain the high biomass of PNF
419 observed in these waters. Anoxic bottom waters were also devoid of *Daphnia* sp. (M. Wauthy et al.,
420 unpublished data) providing to phytoplankton a refuge from grazing. Absence of light, hypoxia and
421 low temperatures further prevent photo-oxidation of algal pigments, preserving them for extended
422 periods (Vallentyne, 1960). Thus some of the Chl-*a* and PNF encountered at the bottom may have

been from dead yet still not degraded cells. Another factor that could have caused bias in very high bottom water Chl-*a* values is the occurrence of chlorophyll-*b* containing green-sulphur bacteria that are known to colonize the anoxic layer of the studied ponds (Rossi et al., 2013), and that may interfere with the spectrophotometric analyses of Chl-*a*. However, green-sulphur bacteria were not found in all ponds with high values of Chl-*a*. In winter, the lack of PP and allocthonous inputs of carbon, and a DOM pool composed by a large fraction of molecules with low aromaticity (low $SUVA_{254}$ and S_{289}) suggest that intensively recycled DOM formed the basal organic carbon pool in thaw ponds.

BP and BB were strongly linked to CDOM originating from a terrestrial source (high $SUVA_{254}$ and a_{320}), indicating a positive link between bacterioplankton and terrestrial carbon (Tranvik, 1988; Crump et al., 2003). These results are in accordance with the experiment from Breton et al. (2009) which showed that bacterioplankton in thaw ponds was more carbon than nutrient-limited (glucose was used as a labile carbon source). On the contrary to several previous studies (Granéli et al., 2004; Säwström et al., 2007; Roiha et al., 2012), the amount of DOC did not seem to control the BP in our study. The studies that reported a positive correlation between DOC and BP have been conducted in summer, when BP and DOC concentrations were highest, but without necessarily taking into account the variability in DOC type, which had a dominant role in our study.

The presence of a mixture of autochthonous and allochthonous carbon may have helped in making the terrestrial carbon available to bacteria. Phytoplankton and macrophytes apparently produced significant amounts of dissolved carbon in surface waters during summer as indicated by the larger S_{289} peak. This carbon is considered more labile (lower molecular weight) and with a higher nutritional value to heterotrophs (Kritzberg et al., 2004; Brett et al., 2009). The availability of high quality phytoplankton carbon during summer possibly enhanced the bacterial use of more recalcitrant terrestrial carbon though the priming effect (Bianchi, 2011), that is a small supplement of nutritionally rich algal cells increasing bacterioplankton terrestrial carbon assimilation.

Correlation between TSS and TP ($r=0.903$ $p<0.001$, $n=15$) indicates that phosphorus was binding to particles, which may be more accessible to attached bacterioplankton than to phytoplankton in summer surface waters where SRP concentrations were low. The high proportion of particle-attached bacterial abundance (62 ± 30 %) and productivity (59 ± 30 %) in thaw ponds suggests that particle attachment is beneficial. Although studies have shown that BP is often nutrient-limited

(Kritzberg et al., 2004; Vrede, 2005), there were no correlation between BP and nutrients in thaw ponds.

One possible additional explanation for the difference between winter and summer BP is the difference in temperature that is known to have a large impact on production (Adams et al., 2010). On the other hand, bacterial communities are known to adapt at low temperatures, and some communities can have multiple temperature maxima (Adams et al., 2010). In our study, the highest BP was found in relatively cool bottom waters. Moreover, bacteria biomass (BB) was not correlated to temperature, although several studies found temperature as a main driver of bacterial biomass (Ochs et al., 1995; Rae and Vincent, 1998). Trophic interactions certainly contributed to the observed patterns in microbial abundance. Rotifers are the dominant zooplankton group in the studied thaw ponds, while the cladoceran community is composed of a few *Daphnia* sp. observed only at the surface (Bégin, 2014). These two zooplankton groups were only found in summer, when they could exert a grazing pressure on bacteria and phytoplankton, but experiments would be needed to confirm the extent of grazing. We tentatively estimated the top-down control of nanoflagellates on bacteria, using the average nanoflagellate ingestion rate of 0.66 pg C $cell^{-1}$ day^{-1} measured for *Dinobryon* sp. in Svalbard (Laybourn-Parry and Marshall, 2003). From these calculations, it seems that nanoflagellate grazing on bacteria could have been efficient enough in late winter when the grazing potential exceeded 100% of the BP, while summer removal estimations corresponded to only 1.7% at the surface and 9.3% at the bottom of the BP, possibly contributing to explaining the accumulation of BB in summer

5 Conclusions

Low light intensity, strong stratification and high concentrations of CDOM in subarctic thaw ponds are the main drivers creating an environment highly beneficial to heterotrophs. We have also shown some important differences in their ecosystem dynamics between winter and summer. Although a high biomass of bacterioplankton is found under the ice, the ponds are producing relatively small amounts of carbon in late winter, likely caused by the lack of fresh carbon inputs and its associated priming effect. Nevertheless, the ponds are accumulating GHG during winter. The relatively high phototrophic biomass and primary production potential encountered under the ice are at the same level as the heterotrophic biomass and production, indicating the importance of mixotrophy in

winter. In summer, fresh primary production and terrestrial carbon inputs enhance the heterotrophic production. Although a higher phototrophic (mixotrophic) biomass is encountered in summer, primary production is restricted by light and space and is significant only at the pond surface, thus the heterotrophic carbon production remains significantly higher. Consequently, GHG continue to accumulate in hypolimnetic waters during this strongly stratified summer period, and are most likely released during the autumnal turnover period, in addition to the constant emissions of GHG throughout the summer from the highly supersaturated surface waters.

6 Acknowledgements

We thank Academy of Finland (grants 119205 and 140775), the Societas Biologica Fennica Vanamo, Maa- ja Vesitekniikan Tuki Ry and the Natural Sciences and Engineering Research Council of Canada for their financial support, and Denis Sarrazin, Paul-Georges Rossi, Frédéric Bouchard, Annabelle Warren, Benoit Ginoux, Catherine Girard and Jonna Kuha for their assistance in the field and laboratory.

7 References

Adams, H. E., Crump, B. C., and Kling, G. W.: Temperature controls on aquatic bacterial production and community dynamics in arctic lakes and streams, Environ. Microbiol., 12, 1319-1333, doi: 10.1111/j.1462-2920.2010.02176.x, 2010.

Arvola, L., Ojala, A., Barbosa, F., and Heaney, S.: Migration behaviour of three cryptophytes in relation to environmental gradients: an experimental approach, Brit. Phyco. J., 26, 361-373, doi: 10.1080/00071619100650331, 1991.

Bastviken, D., Cole, J., Pace, M., and Tranvik, L.: Methane emissions from lakes: Dependence of lake characteristics, two regional assessments, and a global estimate, Global biogeochemical cycles, 18, doi: 10.1029/2004GB002238, 2004.

Bastviken, D., Cole, J. J., Pace, M. L., and Van de Bogert, M. C.: Fates of methane from different lake habitats: connecting whole-lake budgets and CH_4 emissions, J. Geophys. Res.-Biogeo. 2005-2012, 113, doi: 10.1029/2007JG000608, 2008.

Bégin, P. N.: Rotifer abundance, biodiversity and controlling variables in subarctic thermokarst lakes and ponds, M.Sc thesis, Université Laval, Québec, 2014.

Bianchi, T. S.: The role of terrestrially derived organic carbon in the coastal ocean: a changing paradigm and the priming effect, Proc. Natl. Acad. Sci. U. S. A., 108, 19473-19481, doi: 10.1073/pnas.1017982108, 2011.

Bouchard, F., Francus, P., Pienitz, R., and Laurion, I.: Sedimentology and geochemistry of thermokarst ponds in discontinuous permafrost, subarctic Québec, Canada, J. Geophys. Res., 116, doi: 10.1029/2011jg001675, 2011.

519 Bouchard, F., Francus, P., Pienitz, R., Laurion, I., and Feyte, S.: Subarctic thermokarst ponds:
520 Investigating recent landscape evolution and sediment dynamics in thawed permafrost of
521 northern Québec (Canada), Arct. Antarct. Alp. Res., 46, 251-271, doi: 10.1657/1938-4246-
522 46.1.251, 2014.
523 Breton, J., Vallières, C., and Laurion, I.: Limnological properties of permafrost thaw ponds in
524 northeastern Canada, Can. J. Fish. Aquat. Sci., 66, 1635-1648, doi:10.1139/F09-108, 2009.
525 Brett, M. T., Kainz, M. J., Taipale, S. J., and Seshan, H.: Phytoplankton, not allochthonous carbon,
526 sustains herbivorous zooplankton production, P. Natl. Acad. Sci. U.S.A., 106, 21197-21201,
527 doi: 10.1073/pnas.0904129106, 2009.
528 Brinkmann, T., Sartorius, D., and Frimmel, F.: Photobleaching of humic rich dissolved organic
529 matter, Aquat. Sci., 65, 415-424, doi: 10.1007/s00027-003-0670-9, 2003.
530 Campbell, L., Nolla, H. A., and Vaulot, D.: The importance of *Prochlorococcus* to community
531 structure in the central north pacific ocean, Limnol. Oceanogr., 39, 954-961, doi:
532 10.4319/lo.1994.39.4.0954, 1994.
533 Caplanne, S., and Laurion, I.: Effect of chromophoric dissolved organic matter on epilimnetic
534 stratification in lakes, Aquat. Sci., 70, 123-133, doi: 10.1007/s00027-007-7006-0, 2008.
535 Crevecoeur, S., Vincent, W. F., Comte, J., and Lovejoy, C. Bacterial community structure across
536 environmental gradients in permafrost thaw ponds: methanotroph-rich ecosystems, Front.
537 Microbiol., 6, 192. doi: 10.3389/fmicb.2015.00192.
538 Crump, B. C., Kling, G. W., Bahr, M., and Hobbie, J. E.: Bacterioplankton community shifts in an
539 arctic lake correlate with seasonal changes in organic matter source, Appl. Environ.
540 Microbiol., 69, 2253-2268, doi: 10.1128/aem.69.4.2253-2268.2003, 2003.
541 Del Giorgio, P., and Davis, J.: Patterns in dissolved organic matter lability and consumption across
542 aquatic ecosystems, in: Aquatic ecosystems: Interactivity of dissolved organic matter, edited
543 by : Findlay, S. E. G., and Sinsabaugh, R. E., Academic press, San Diego, ca, 399-424, 2002.
544 Del Giorgio, P. A., and Cole, J. J.: Bacterial growth efficiency in natural aquatic systems, Annu.
545 Rev. Ecol. Syst., 503-541, 1998.
546 Deshpande, B. N., MacIntyre, S., Matveev, A., and Vincent, W. F.: Oxygen dynamics in permafrost
547 thaw lakes: anaerobic bioreactors in the Canadian subarctic, Limnol. Oceanogr., 2015.

548 Doxaran, D., Cherukuru, R. C. N., and Lavender, S. J.: Estimation of surface reflection effects on
549 upwelling radiance field measurements in turbid waters, J. Opt. A-Pure Appl. Op., 6, 690-
550 697, Pii S1464/4258(04)75616-0, doi: 10.1088/1464-4258/6/7/006, 2004.
551 Dupont, C.: Microbial diversity of thermokarst pond and their greenhouse gas production, M.Sc
552 thesis, Institut national de la recherche scientifique, Université du Québec, Québec, 2008.
553 Eller, G., Kanel, L., and Kruger, M.: Cooccurrence of aerobic and anaerobic methane oxidation in
554 the water column of lake Plußsee, Appl. Environ. Microbiol., 71, 8925-8928, doi:
555 10.1128/AEM.71.12.8925-8928.2005, 2005.
556 Fendinger, N. J., Adams, D. D., and Glotfelty, D. E.: The role of gas ebullition in the transport of
557 organic contaminants from sediments, Sci. Total. Environ., 112, 189-201, doi 10.1016/0048-
558 9697(92)90187-W, 1992.
559 Galgani, L., Tognazzi, A., Rossi, C., Ricci, M., Galvez, J. A., Dattilo, A. M., Cozar, A., Bracchini,
560 L., and Loiselle, S. A.: Assessing the optical changes in dissolved organic matter in humic
561 lakes by spectral slope distributions, J. Photoch. Photobio. B, 102, 132-139, doi:
562 10.1016/j.jphotobiol.2010.10.001, 2011.
563 Granéli, W., Bertilsson, S., and Philibert, A.: Phosphorus limitation of bacterial growth in high
564 arctic lakes and ponds, Aquat. Sci., 66, 430-439, doi: 10.1007/s00027-004-0732-7, 2004.
565 Guérin, F., Abril, G., Richard, S., Burban, B., Reynouard, C., Seyler, P., and Delmas, R.: Methane
566 and carbon dioxide emissions from tropical reservoirs: significance of downstream rivers,
567 Geophys. Res. Lett., 33, doi: 10.1029/2006gl027929, 2006.
568 Guillemette, F., and del Giorgio, P. A.: Reconstructing the various facets of dissolved organic
569 carbon bioavailability in freshwater ecosystems, Limnol. Oceanogr., 56, 734-748, doi:
570 10.4319/lo, 2011.
571 Hamilton, P. B., Gajewski, K., Atkinson, D. E., and Lean, D. R. S.: Physical and chemical
572 limnology of 204 lakes from the Canadian arctic archipelago, Hydrobiologia, 457, 133-148,
573 doi 10.1023/A:1012275316543, 2001.
574 Hudson, J. J., Dillon, P. J., and Somers, K. M.: Long-term patterns in dissolved organic carbon in
575 boreal lakes: the role of incident radiation, precipitation, air temperature, southern oscillation
576 and acid deposition, Hydrol. Earth. Syst. Sc., 7, 390-398, doi: 10.5194/hess-7-390-2003,
577 2003.

578 Jassby, A. D., and Platt, T.: Mathematical formulation of the relationship between photosynthesis
579 and light for phytoplankton, Limnol. Oceanogr., 21, 540-547, 1976.
580 Jones, R. I.: Advantages of diurnal vertical migrations to phytoplankton in sharply stratified, humic
581 forest lakes, Arch. Hydrobiol., 120, 257-266, 1991.
582 Jones, R. I.: Mixotrophy in planktonic protists: an overview, Freshwat. Biol., 45, 219-226, doi:
583 10.1046/j.1365-2427.2000.00672.x, 2000.
584 Juutinen, S., Rantakari, M., Kortelainen, P., Huttunen, J. T., Larmola, T., Alm, J., Silvola, J., and
585 Martikainen, P. J.: Methane dynamics in different boreal lake types, Biogeosciences, 6, 209-
586 223, doi: 10.5194/bg-6-209-2009, 2009.
587 Kling, G. W., Kipphut, G. W., and Miller, M. C.: The flux of CO2 and CH_4 from lakes and rivers in
588 arctic Alaska, Hydrobiologia, 240, 23-36, doi 10.1007/Bf00013449, 1992.
589 Kortelainen, P., Rantakari, M., Huttunen, J. T., Mattsson, T., Alm, J., Juutinen, S., Larmola, T.,
590 Silvola, J., and Martikainen, P. J.: Sediment respiration and lake trophic state are important
591 predictors of large CO_2 evasion from small boreal lakes, Global Change Biol., 12, 1554-1567,
592 doi 10.1111/j.1365-2486.2006.01167.x, 2006.
593 Kritzberg, E. S., Cole, J. J., Pace, M. L., Granéli, W., and Bade, D. L.: Autochthonous versus
594 allochthonous carbon sources of bacteria: results from whole-lake ^{13}C addition experiments,
595 Limnol. Oceanogr., 49, 588-596, doi: 10.4319/lo.2004.49.2.0588, 2004.
596 Laurion, I., Vincent, W. F., MacIntyre, S., Retamal, L., Dupont, C., Francus, P., and Pienitz, R.:
597 Variability in greenhouse gas emissions from permafrost thaw ponds, Limnol. Oceanogr., 55,
598 doi: 115-133, doi: 10.4319/lo.2010.55.1.0115, 2010.
599 Laurion, I., and Mladenov, N.: Dissolved organic matter photolysis in Canadian arctic thaw ponds,
600 Environ. Res. Lett., 8, 035026, Artn 035026, doi 10.1088/1748-9326/8/3/035026, 2013.
601 Laws, E. A., Popp, B. N., Bidigare, R. R., Kennicutt, M. C., and Macko, S. A.: Dependence of
602 phytoplankton carbon isotopic composition on growth rate and $[CO_2]$aq: theoretical
603 considerations and experimental results, Geochim. Cosmochim. Acta, 59, 1131-1138, doi:
604 10.1016/0016-7037(95)00030-4, 1995.
605 Laybourn-Parry, J., and Marshall, W. A.: Photosynthesis, mixotrophy and microbial plankton
606 dynamics in two high arctic lakes during summer, Polar Biol., 26, 517-524, doi:
607 10.1007/s00300-003-0514-z, 2003.

608 Lindell, M. J., Graneli, W., and Tranvik, L. J.: Enhanced bacterial-growth in response to
609 photochemical transformation of dissolved organic-matter, Limnol. Oceanogr., 40, 195-199,
610 doi: 10.4319/lo.1995.40.1.0195, 1995.
611 Lizotte, M. P.: Phytoplankton and primary production, in: Polar lakes and rivers: limnology of
612 arctic and antarctic aquatic ecosystems, edited by: Vincent, W. F. and Laybourn-Parry, J.,
613 Oxford University Press, Oxford, UK, pp. 197–212, 2008.
614 Loiselle, S. A., Bracchini, L., Cozar, A., Dattilo, A. M., Tognazzi, A., and Rossi, C.: Variability in
615 photobleaching yields and their related impacts on optical conditions in subtropical lakes, J.
616 Photoch. Photobio. B, 95, 129-137, doi: 10.1016/j.jphotobiol.2009.02.002, 2009.
617 Maloney, K. O., Morris, D. P., Moses, C. O., and Osburn, C. L.: The role of iron and dissolved
618 organic carbon in the absorption of ultraviolet radiation in humic lake water,
619 Biogeochemistry, 75, 393-407, doi: 10.1007/s10533-005-1675-3, 2005.
620 Marshall, J. D., Brooks, J. R., and Lajtha, K.: Sources of variation in the stable isotopic composition
621 of plants, Stable isotopes in ecology and environmental science, 22-60, doi:
622 10.1002/9780470691854.ch2, 2007.
623 Medeiros, A. S., Biastoch, R. G., Luszczek, C. E., Wang, X. A., Muir, D. C. G., and Quinlan, R.:
624 Patterns in the limnology of lakes and ponds across multiple local and regional environmental
625 gradients in the eastern Canadian arctic, Inland Waters, 2, 59-76, doi 10.5268/Iw-2.2.427,
626 2012.
627 Mitchell, B. G., Kahru, M., Wieland, J., and Stramska, M.: Determination of spectral absorption
628 coefficients of particles, dissolved material and phytoplankton for discrete water samples,
629 Ocean optics protocols for satellite ocean color sensor validation, Revision, 3, 231-257, 2002.
630 Moal, J., Martinjezequel, V., Harris, R. P., Samain, J. F., and Poulet, S. A.: Interspecific and
631 intraspecific variability of the chemical-composition of marine-phytoplankton, Oceanol. Acta,
632 doi: 10, 339-346, 1987.
633 Negandhi, K., Laurion, I., Whiticar, M. J., Galand, P. E., Xu, X., and Lovejoy, C.: Small thaw
634 ponds: an unaccounted source of methane in the Canadian high arctic, PLoS One, 8, doi:
635 e78204, 10.1371/journal.pone.0078204, 2013.
636 Nush, E.: Comparison of different methods for chlorophyll and phaeopigment determination, Arch.
637 Hydrobiol. Beih, 14, 14-36, 1980.

638 Ochs, C. A., Cole, J. J., and Likens, G. E.: Population-dynamics of bacterioplankton in an
639 oligotrophic lake, J. Plankton. Res., 17, 365-391, doi: 10.1093/plankt/17.2.365, 1995.
640 Olrik, K.: Ecology of mixotrophic flagellates with special reference to chrysophyceae in Danish
641 lakes, Hydrobiologia, 370, 329-338, doi: 10.1023/A:1017045809572, 1998.
642 Pienitz, R., Smol, J. P., and Lean, D. R. S.: Physical and chemical limnology of 59 lakes located
643 between the southern Yukon and the Tuktoyaktuk peninsula, Northwest Territories (Canada),
644 Can. J. Fish. Aquat. Sci., 54, 330-346, doi: 10.1139/cjfas-54-2-330, 1997.
645 Platt, T., Gallegos, C. L., and Harrison, W. G.: Photoinhibition of photosynthesis in natural
646 assemblages of marine-phytoplankton, J. Mar. Res., 38, 687-701, 1980.
647 Posch, T., Loferer-Krossbacher, M., Gao, G., Alfreider, A., Pernthaler, J., and Psenner, R.:
648 Precision of bacterioplankton biomass determination: a comparison of two fluorescent dyes,
649 and of allometric and linear volume-to-carbon conversion factors, Aquat. Microb. Ecol., 25,
650 55-63, doi: 10.3354/ame025055, 2001.
651 Putt, M., and Stoecker, D. K.: An experimentally determined carbon: volume ratio for marine
652 “oligotrichous” ciliates from estuarine and coastal waters, Limnol. Oceanogr., 34, 1097-1103,
653 1989.
654 Rae, R., and Vincent, W. F.: Phytoplankton production in subarctic lake and river ecosystems:
655 development of a photosynthesis-temperature-irradiance model, J. Plankton Res., 20, 1293-
656 1312, doi: 10.1093/plankt/20.7.1293, 1998.
657 Rautio, M., Dufresne, F., Laurion, I., Bonilla, S., Vincent, W. F., and Christoffersen, K. S.: Shallow
658 freshwater ecosystems of the circumpolar arctic, Ecoscience, 18, 204-222, doi 10.2980/18-3-
659 3463, 2011a.
660 Rautio, M., Mariash, H., and Forsström, L.: Seasonal shifts between autochthonous and
661 allochthonous carbon contributions to zooplankton diets in a subarctic lake, Limnol.
662 Oceanogr., 56, 1513-1524, doi: 10.4319/lo.2011.56.4.1513, 2011b.
663 Roehm, C. L., Giesler, R., and Karlsson, J.: Bioavailability of terrestrial organic carbon to lake
664 bacteria: the case of a degrading subarctic permafrost mire complex, J. Geophys. Res.-
665 Biogeo., 114, Artn G03006, doi: 10.1029/2008jg000863, 2009.
666 Roiha, T., Tiirola, M., Cazzanelli, M., and Rautio, M.: Carbon quantity defines productivity while
667 its quality defines community composition of bacterioplankton in subarctic ponds, Aquat.
668 Sci., 74, 513-525, doi: 10.1007/s00027-011-0244-1, 2012.

669 Rossi, P. G., Laurion, I., and Lovejoy, C.: Distribution and identity of bacteria in subarctic
670 permafrost thaw ponds, Aquat. Microb. Ecol., 69, 231-245, doi: 10.3354/ame01634, 2013.
671 Salonen, K., Jones, R. I., and Arvola, L.: Hypolimnetic phosphorus retrieval by diel vertical
672 migrations of lake phytoplankton, Freshwat. Biol., 14, 431-438, doi: 10.1111/j.1365-
673 2427.1984.tb00165.x, 1984.
674 Salonen, K., and Rosenberg, M.: Advantages from diel vertical migration can explain the
675 dominance of *Gonyostomum semen* (Raphidophyceae) in a small, steeply-stratified humic
676 lake, J. Plankton Res., 22, 1841-1853, doi: 10.1093/plankt/22.10.1841, 2000.
677 Säwström, C., Laybourn-Parry, J., Granéli, W., and Anesio, A. M.: Heterotrophic bacterial and viral
678 dynamics in arctic freshwaters: results from a field study and nutrient-temperature
679 manipulation experiments, Polar Biol., 30, 1407-1415, doi: 10.1007/s00300-007-0301-3,
680 2007.
681 Squires, M. M., and Lesack, L. F. W.: Spatial and temporal patterns of light attenuation among
682 lakes of the Mackenzie Delta, Freshwater Biol., 48, 1–20, doi: 10.1046/j.1365-
683 2427.2003.00960.x, 2003.
684 Selinummi, J., Seppälä, J., Yli-Harja, O., and Puhakka, J. A.: Software for quantification of labeled
685 bacteria from digital microscope images by automated image analysis, BioTechniques, 39,
686 859-863, 2005.
687 Shirokova, L. S., Pokrovsky, O. S., Kirpotin, S. N., Desmukh, C., Pokrovsky, B. G., Audry, S., and
688 Viers, J.: Biogeochemistry of organic carbon, CO_2, CH_4, and trace elements in thermokarst
689 water bodies in discontinuous permafrost zones of western Siberia, Biogeochemistry, 113,
690 573-593, doi: 10.1007/s10533-012-9790-4, 2013.
691 Simon, M., and Azam, F.: Protein-content and protein-synthesis rates of planktonic marine-bacteria,
692 Mar. Ecol. Prog. Ser., 51, 201-213, doi: 10.3354/meps051201, 1989.
693 Sivan, O., Adler, M., Pearson, A., Gelman, F., Bar-Or, I., John, S. G., and Eckert, W.: Geochemical
694 evidence for iron-mediated anaerobic oxidation of methane, Limnol. Oceanogr., 56, 1536-
695 1544, doi: 10.4319/lo.2011.56.4.1536, 2011.
696 Skovgaard, A., Hansen, P. J., and Stoecker, D. K.: Physiology of the mixotrophic dinoflagellate
697 *Fragilidium subglobosum*. I. Effects of phagotrophy and irradiance on photosynthesis and
698 carbon content, Mar. Ecol. Prog. Ser., 201, 129-136, doi: 10.3354/meps201129, 2000.

699 Smith, D. C., and Azam, F.: A simple, economical method for measuring bacterial protein synthesis
700 rates in seawater using ^{3}H-leucine, Mar. Microb. Food Webs, 6, 107-114, 1992.
701 Teodoru, C. R., del Giorgio, P. A., Prairie, Y. T., and Camire, M.: Patterns in pCO_2 in boreal
702 streams and rivers of northern Quebec, Canada, Global Biogeochemical Cycles, 23, doi:
703 10.1029/2008gb003404, 2009.
704 Tranvik, L. J.: Availability of dissolved organic carbon for planktonic bacteria in oligotrophic lakes
705 of differing humic content, Microb. Ecol., 16, 311-322, doi: 10.1007/BF02011702, 1988.
706 Tranvik, L. J., Downing, J. A., Cotner, J. B., Loiselle, S. A., Striegl, R. G., Ballatore, T. J., Dillon,
707 P., Finlay, K., Fortino, K., Knoll, L. B., Kortelainen, P. L., Kutser, T., Larsen, S., Laurion, I.,
708 Leech, D. M., McCallister, S. L., McKnight, D. M., Melack, J. M., Overholt, E., Porter, J. A.,
709 Prairie, Y., Renwick, W. H., Roland, F., Sherman, B. S., Schindler, D. W., Sobek, S.,
710 Tremblay, A., Vanni, M. J., Verschoor, A. M., von Wachenfeldt, E., and Weyhenmeyer, G.
711 A.: Lakes and reservoirs as regulators of carbon cycling and climate, Limnol. Oceanogr., 54,
712 2298-2314, doi: 10.4319/lo.2009.54.6_part_2.2298, 2009.
713 Vallentyne, J.: Fossil pigments, Comparative biochemistry of photoreactive systems, 83-105, 1960.
714 Walter Anthony, K. M., Zimov, S. A., Grosse, G., Jones, M. C., Anthony, P. M., Chapin, F. S., 3rd,
715 Finlay, J. C., Mack, M. C., Davydov, S., Frenzel, P., and Frolking, S.: A shift of thermokarst
716 lakes from carbon sources to sinks during the Holocene epoch, Nature, 511, 452-456, doi:
717 10.1038/nature13560, 2014.
718 Verity, P. G., Robertson, C. Y., Tronzo, C. R., Andrews, M. G., Nelson, J. R., and Sieracki, M. E.:
719 Relationships between cell-volume and the carbon and nitrogen-content of marine
720 photosynthetic nanoplankton, Limnol. Oceanogr., 37, 1434-1446, 1992.
721 Vonk, J. E., Sanchez-Garcia, L., van Dongen, B. E., Alling, V., Kosmach, D., Charkin, A.,
722 Semiletov, I. P., Dudarev, O. V., Shakhova, N., Roos, P., Eglinton, T. I., Andersson, A., and
723 Gustafsson, O.: Activation of old carbon by erosion of coastal and subsea permafrost in arctic
724 Siberia, Nature, 489, 137-140, doi: 10.1038/nature11392, 2012.
725 Vonk, J. E., Tank, S. E., Bowden, W. B., Laurion, I., Vincent, W. F., Alekseychik, P., Amyot, M.,
726 Billet, M. F., Canário, J., Cory, R. M., Deshpande, B. N., Helbig, M., Jammet, M., Karlsson,
727 J., Larouche, J., MacMillan, G., Rautio, M., Walter Anthony, K. M., and Wickland, K. P.
728 Reviews and Syntheses: Effects of permafrost thaw on arctic aquatic ecosystems,
729 Biogeosciences Discuss., 12, 10719-10815, 2015. doi:10.5194/bgd-12-10719-2015.

730 Vrede, K.: Nutrient and temperature limitation of bacterioplankton growth in temperate lakes,
731 Microb. Ecol., 49, 245-256, doi: 10.1007/s00248-004-0259-4, 2005.
732 Walter, K. M., Zimov, S. A., Chanton, J. P., Verbyla, D., and Chapin, F. S.: Methane bubbling from
733 Siberian thaw lakes as a positive feedback to climate warming, Nature, 443, 71-75, doi:
734 10.1038/nature05040, 2006.
735 Watanabe, S., Laurion, I., Chokmani, K., Pienitz, R., and Vincent, W. F.: Optical diversity of thaw
736 ponds in discontinuous permafrost: a model system for water color analysis, J. Geophys. Res.-
737 Biogeo., 116, Artn G02003, doi: 10.1029/2010jg001380, 2011.
738 Weishaar, J. L., Aiken, G. R., Bergamaschi, B. A., Fram, M. S., Fujii, R., and Mopper, K.:
739 Evaluation of specific ultraviolet absorbance as an indicator of the chemical composition and
740 reactivity of dissolved organic carbon, Environ. Sci. Technol., 37, 4702-4708, doi:
741 10.1021/es030360x, 2003.
742 Xiao, Y. H., Sara-Aho, T., Hartikainen, H., and Vähätalo, A. V.: Contribution of ferric iron to light
743 absorption by chromophoric dissolved organic matter, Limnol. Oceanogr., 58, 653-662, doi
744 10.4319/lo.2013.58.2.0653, 2013.
745

746 **Figure captions**

747

748 Figure 1. Summer temperature and oxygen profiles from sampled ponds.

749

750 Figure 2. Absorption spectral slope curve (S_λ) of dissolved organic matter as an indicator of the
751 presence of algal-derived carbon (peak at S_{289}) and terrestrial carbon (steady increase in the slopes
752 from 260-390 nm).

753

754 Figure 3. Seasonal changes in the biomass of phototrophic picoplankton (PPA), pigmented
755 nanoflagellates (PNF), bacteria (BB), and heterotrophic nanoflagellates (HNF). Error bars
756 represent standard errors.

757

758 Figure 4. a) Seasonality in pond environmental variables illustrated with principal component
759 analysis during late winter (triangles), summer surface (diamonds) and summer bottom (crosses). b)
760 Spearman correlation coefficients between biological variables and principal components 1 (x-axis)
761 and 2 (y-axis). BP=bacterial production, BB=bacterial biomass, HNF=heterotrophic nanoflagellate
762 biomass, PP=primary production, PNF=pigmented nanoflagellate biomass, and PPA=phototrophic
763 picoplankton biomass.

764

765

766 **Table 1.** Limnological properties of the subarctic ponds sampled in late winter (W) and during
767 summer at the surface (S) and bottom (B) of the water column, including pH, conductivity
768 (Cond.), total phosphorus (TP), total nitrogen (TN), soluble reactive phosphorus (SRP), total
769 suspended solids (TSS), particulate organic carbon (POC) and iron (Fe).

Site	pH	Cond. ($\mu S\ cm^{-1}$)	TP ($\mu g\ L^{-1}$)	TN ($\mu g\ L^{-1}$)	SRP ($\mu g\ L^{-1}$)	TSS ($mg\ L^{-1}$)	POC ($mg\ L^{-1}$)	Fe ($mg\ L^{-1}$)
Winter								
KWK 2	6.6	60	61.9	957.4	20.8	2.7	0.8	na
KWK 6	6.8	49	50.6	687.8	7.7	3.7	1.1	na
KWK 12	6.6	46	73.2	1038.4	18.4	4.1	1.2	na
KWK 20	6.7	52	180.7	1301.6	47.1	53.9	16.6	na
KWK 23	6.4	42	119.3	802.7	33,9	23.5	6.8	na
Summer surface								
KWK 2	7.4	38	34.9	289.3	1.2	3.4	0.9	0.3
KWK 6	6.9	61	43.9	227.9	0.9	7.2	2.3	0.2
KWK 12	7.3	36	23.9	311.9	0.7	2.6	0.9	0.3
KWK 20	7.5	47	92.6	263.4	7.1	14.2	1.8	0.5
KWK 23	7.1	48	78.0	227.9	5.7	16.1	2.1	0.4
Summer bottom								
KWK 2	6.2	200	341.5	496.1	1.5	27.7	4.4	2.5
KWK 6	6.2	265	197.7	389.4	na	13.6	2.3	1.1
KWK 12	6.1	247	207.1	447.6	1.0	37.0	8.8	2.9
KWK 20	6.0	155	377.0	289.3	73.8	85.8	5.7	5.1
KWK 23	6.2	102	431.8	266.7	45.7	126.8	7.8	4.1

770
771

Table 2. Concentrations of carbon dioxide (CO_2), methane (CH_4), and dissolved organic carbon (DOC), and dissolved organic matter (DOM) optical properties, including absorption coefficient of DOM at 320 nm (a_{320}), specific UV-absorbance index ($SUVA_{254}$), and absorption spectral slopes at 289 nm (S_{289}) and 382 nm (S_{382}), of subarctic pond water sampled in late winter and during summer at the surface and bottom of the water column.

Site	CO_2 (µM)	CH_4 (µM)	DOC (mg L^{-1})	a_{320} (m^{-1})	$SUVA_{254}$ (L mg C^{-1} m^{-1})	S_{289} (nm^{-1})	S_{382} (nm^{-1})
Winter							
KWK 2	316	14.1	7.7	8.5	0.9	0.0099	0.0155
KWK 6	354	5.1	5.2	3.0	0.5	0.0112	0.0122
KWK 12	215	2.4	10.5	9.5	0.8	0.0105	0.0154
KWK 20	na	na	10.3	8.1	0.8	0.0125	0.0130
KWK 23	357	2.5	7.9	6.6	0.8	0.0124	0.0123
Summer surface							
KWK 2	72	0.6	5.6	26.4	4.7	0.0141	0.0169
KWK 6	27	0.5	4.1	11.8	3.4	0.0162	0.0135
KWK 12	55	0.3	6.0	26.5	4.5	0.0142	0.0170
KWK 20	71	0.3	7.1	38.9	6.1	0.0145	0.0156
KWK 23	53	0.3	6.3	30.7	5.4	0.0150	0.0161
Summer bottom							
KWK 2	na	na	6.1	51.5	6.7	0.0109	0.0156
KWK 6	422	145.2	4.2	21.4	4.3	0.0125	0.0173
KWK 12	761	259.0	7.4	67.9	7.4	0.0111	0.0173
KWK 20	815	311.9	9.3	115.6	9.8	0.0107	0.0172
KWK 23	570	131.6	7.5	94.5	10.2	0.0109	0.0171

Table 3. Phototrophic and heterotrophic properties of subarctic pond water sampled in late winter and during summer at the surface and bottom of the water column, including chlorophyll-*a* concentration (Chl-*a*), maximum photosynthesis parameter (P_{max}), *in situ* primary production (PP), pigmented nanoflagellate abundance (PNF), phototrophic picoplankton abundance (PPA), bacterial production (BP), bacterial respiration (BR), bacterial abundance (BA) and heterotrophic nanoflagellate abundance (HNF).

Site	Chl-*a* ($\mu g\ L^{-1}$)	P_{max} (mg C m^{-3} d^{-1})	PP (mg C m^{-3} d^{-1})	PNF ($\times 10^6\ L^{-1}$)	PPA ($\times 10^5\ mL^{-1}$)	BP (mg C m^{-3} d^{-1})	BR (mg C m-3 d^{-1})	BA ($\times 10^6\ mL^{-1}$)	HNF ($\times 10^6\ L^{-1}$)
Winter									
KWK 2	2.8	1.2	0	33.0	0.2	0.2	1.3	4.2	2.0
KWK 6	9.9	0.8	0	51.0	0.9	0.5	2.2	11.2	3.3
KWK 12	11.5	5.8	0	29.1	0.7	0.3	1.6	2.5	2.4
KWK 20	2.8	0.8	0	6.3	0.2	0.8	3.0	8.7[a]	2.4
KWK 23	0.8	1.5	0	10.0	0.1	0.4	2.0	3.7	0.3
Summer surface									
KWK 2	5.4	4.5	2.6	16.3	3.3	27.2	25.7	13.3	0.0
KWK 6	13.4	27.9	15.3	20.0	4.2	37.4	31.2	11.3	0.8
KWK 12	2.2	5.9	3.2	28.8	0.9	31.2	27.9	9.6	0.7
KWK 20	14.3	59.0	26.4	33.1	17.3	15.2	18.0	14.8	1.9
KWK 23	12.3	55.6	15.6	35.0	3.8	45.9	35.3	12.7	0.4
Summer bottom									
KWK 2	180.2	na	0.8	149.6	9.4	57.6	40.5	35.7	26.2
KWK 6	87.2	na	4.2	201.6	3.0	39.0	32.0	14.3	6.3
KWK 12	158.9	na	0.3	72.5	26.8	48.8	36.6	38.0	3.7
KWK 20	203.4	na	0.3	na	4.0	39.1	32.0	27.2	na
KWK 23	37.1	na	0.0	4.5	6.2	23.0	23.2	24.3	0.6

[a] BA was calculated from DAPI-stained microscope slide

787 **Table 4.** Spearman correlations between biological and environmental variables. Only statistically
788 significant correlations are given.

Biological variable	Environmental variable	n	r	p
Bacteria production (BP)	Temperature	15	0.600	0.018
	TN	15	-0.524	0.045
	a_{320}	15	0.704	0.003
	$SUVA_{254}$	15	0.699	0.004
	S382	15	0.633	0.011
Bacteria biomass (BB)	O_2	15	0.555	0.049
	Conductivity	15	0.668	0.007
	TP	15	0.600	0.018
	TSS	15	0.521	0.046
	Fe	10	0.879	0.001
	CH_4	13	0.588	0.035
	a_{320}	15	0.825	<0.001
	$SUVA_{254}$	15	0.857	<0.001
	S382	15	0.716	0.003
HNF	Conductivity	15	0.657	0.011
	CH_4	15	0.636	0.026
Primary production (PP)	Temperature	10	0.896	<0.001
	SRP	10	-0.662	0.007
	TN	10	-0.827	<0.001
	DOC	10	-0.610	0.016
	$SUVA_{254}$	10	0.533	0.041
	S289	10	0.732	0.002
PNF	SRP	14	-0.732	0.003
	DOC	14	-0.647	0.012
PPA	TN	15	-0.665	0.007
	a_{320}	15	0.825	<0.001
	$SUVA_{254}$	15	0.717	0.003
	S382	15	0.564	0.029

789 **Figure 1.**

790

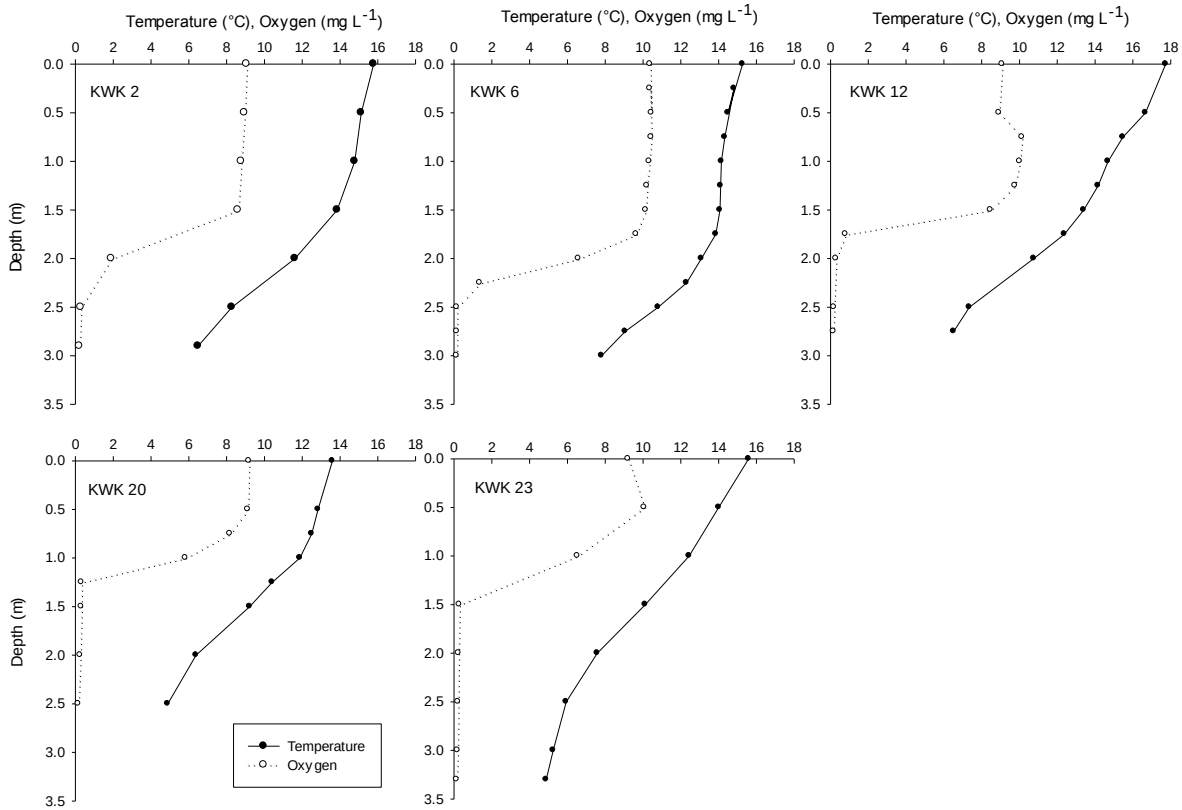

791

792

793

794

795 **Figure 2.**

796

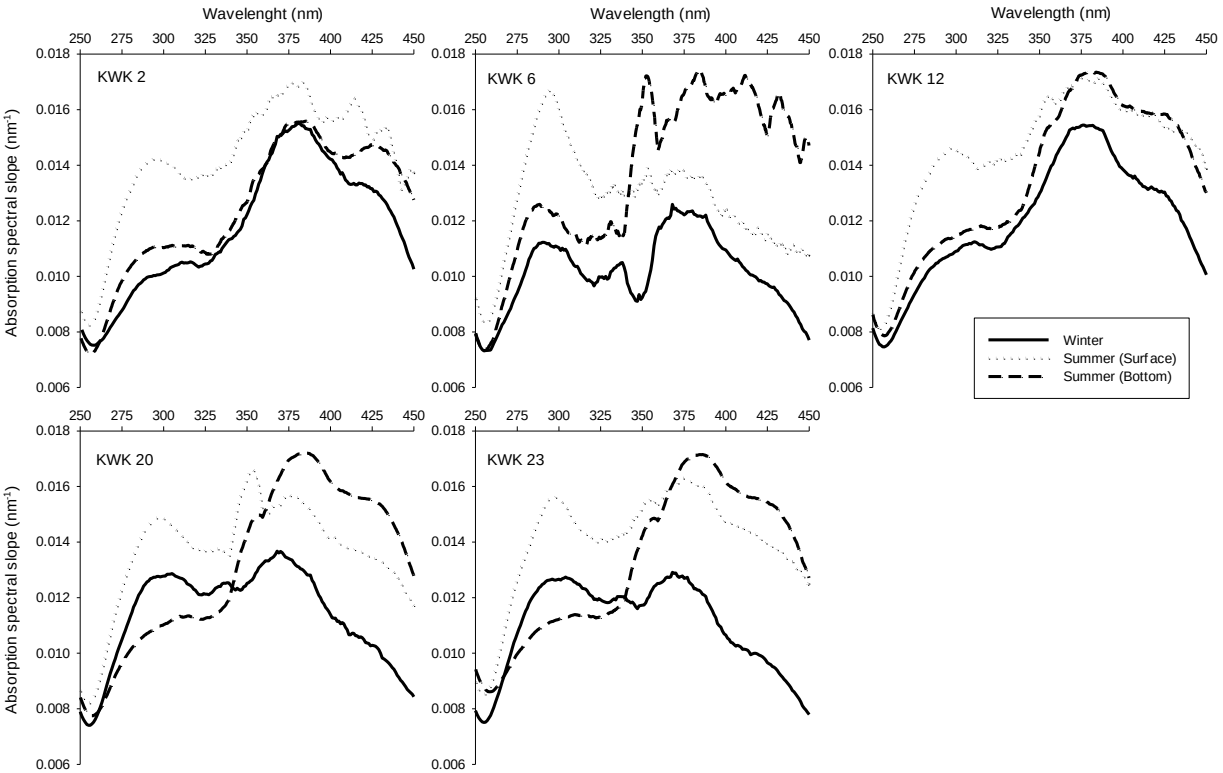

797

798

799

800 **Figure 3.**

801

802

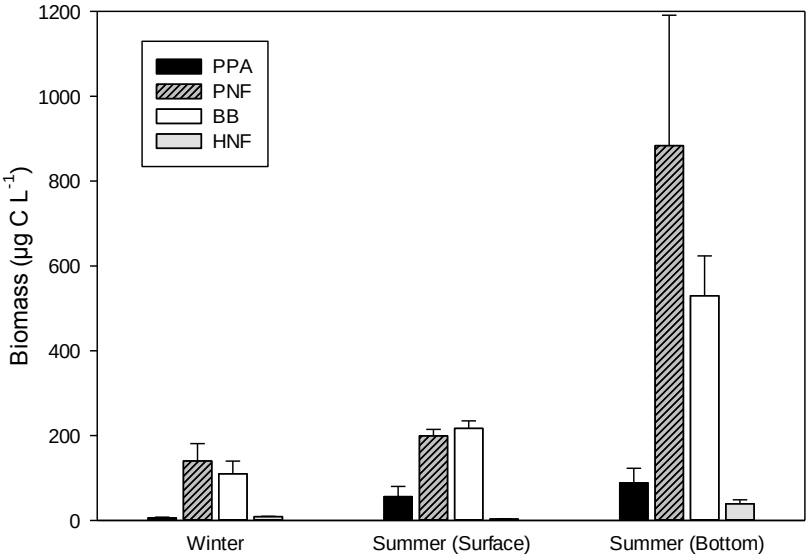

803

804

Figure 4.

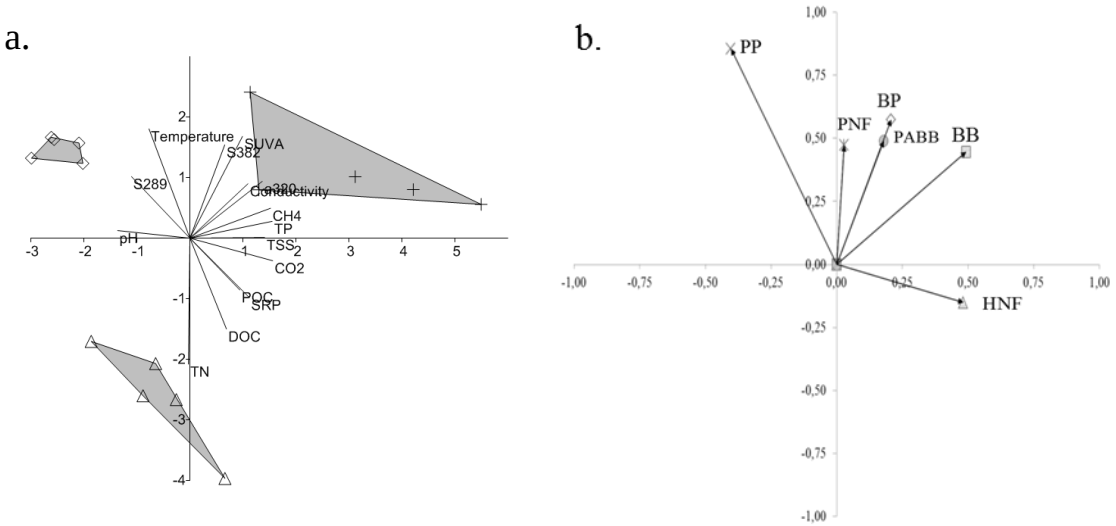
a.
Temperature
SUVA
S382
S289
Conductivity
CH4
TP
pH
TSS
CO2
POC
SRP
DOC
TN
b.
PP
BP
PNF
PABB
BB
HNF

Appendix A:

Table A1. Particle attachment of bacterioplankton in winter, during summer at the surface and bottom of ponds, including sonicated bacterial abundance (BA_T) representing the total abundance, bacterial abundance before sonication (BA_{FL}) representing free-living bacteria, proportion of particle-attached bacteria (BA_P), total bacterial production (BP; as in Table 3), filtered (3µm) bacterial production (BP_{FL}) and proportion of particle attached bacterial production (BP_P).

Site	BA_T ($\times 10^6$ mL^{-1})	BA_{FL} ($\times 10^6$ mL^{-1})	BA_P (%)	BP (mg C m^{-3} d^{-1})	BP_{FL} (mg C m^{-3} d^{-1})	BP_P (%)
Winter						
KWK 2	4.2	0.8	81	0.2	0.1	54
KWK 6	11.2	3.2	72	0.5	0.2	54
KWK 12	2.5	0.5	79	0.3	0.2	48
KWK 20	na	na	na	0.8	0.4	47
KWK 23	3.7	1.4	62	0.4	0.4	7
Summer surface						
KWK 2	13.3	5.8	57	27.2	4.7	83
KWK 6	11.3	8.5	24	37.4	3.3	91
KWK 12	9.6	6.0	37	31.2	17.4	56
KWK 20	14.8	4.1	73	15.2	7.0	54
KWK 23	12.7	7.7	40	45.9	18.6	60
Summer bottom						
KWK 2	35.7	11.3	68	57.6	1.7	97
KWK 6	14.3	8.3	42	39.0	1.5	96
KWK 12	38.0	11.2	70	48.8	26.0	47
KWK 20	27.2	3.7	86	39.1	1.0	97
KWK 23	24.3	4.2	83	23.0	26.6	0